

## Mechanisms of electroconductivity in $\text{Na}_{0.5}\text{Bi}_{0.5}\text{TiO}_3$ single crystals

T.V. Kruzina<sup>1</sup>, V.M. Sidak<sup>1</sup>, M.P. Trubitsyn<sup>1</sup>, S.A. Popov<sup>1</sup>, J. Suchanicz<sup>2</sup>

<sup>1</sup>*Oles Honchar Dnipropetrovsk National University, pr. Gagarina 72,  
49010 Dnipropetrovsk, Ukraine*

<sup>2</sup>*Institute of Physics, Pedagogical University, ul. Podchorazych 2,  
30-84 Krakow, Poland*

The complex impedance spectra  $Z^*(\omega)$  of  $\text{Na}_{0.5}\text{Bi}_{0.5}\text{TiO}_3$  single crystals were studied in the temperature interval 600-900 K and in the frequency range  $5\text{-}5 \cdot 10^5$  Hz. Experimental data are presented as diagrams in the complex ( $Z'$ - $Z''$ ) plane and discussed on the basis of the equivalent circuits approach. In the studied temperature-frequency diapason the hodographs consist of two arcs and are described by using an equivalent circuit, containing two serially connected parallel RC circuits. Shift of the arcs centers downward from  $Z'$  axis, caused by distribution of the impedance relaxation times  $\tau$ , is accounted by substitution of usual capacities for generalized ones. The high-frequency arc on the hodographs is associated with conductivity in the bulk of the sample. The low-frequency arc reflects the charge transfer in the near electrode regions.

**Keywords:** sodium bismuth titanate  $\text{Na}_{0.5}\text{Bi}_{0.5}\text{TiO}_3$ , impedance spectroscopy, electroconductivity.

В температурній області 600-900 К і в частотному діапазоні  $5 - 5 \cdot 10^5$  Гц вивчені спектри комплексного імпедансу  $Z^*(\omega)$  монокристалів  $\text{Na}_{0.5}\text{Bi}_{0.5}\text{TiO}_3$ . Експериментальні дані представлені в вигляді діаграм на комплексній площині ( $Z'$ - $Z''$ ) та обговорюються на підставі методу еквівалентних схем заміщення. Для вивченого температурно- частотного діапазону годографи містять дві дуги та описуються з використанням еквівалентної схеми, що складається з двох послідовно з'єднаних паралельних RC ланцюжків. Зсув центрів дуг вниз від осі  $Z'$ , обумовлений розподілом часів релаксації  $\tau$  імпедансу, враховано заміною звичайних ємностей узагальненими. Високочастотна дуга на годографах зіставлена провідності в об'ємі зразка. Низькочастотна дуга відображає перенесення заряду в приелектродних областях.

**Ключевые слова:** натрий-висмутитовый титанат  $\text{Na}_{0.5}\text{Bi}_{0.5}\text{TiO}_3$ , импедансная спектроскопия, электропроводность.

В температурній області 600-900 К і в частотному діапазоні  $5 - 5 \cdot 10^5$  Гц вивчені спектри комплексного імпедансу  $Z^*(\omega)$  монокристалів  $\text{Na}_{0.5}\text{Bi}_{0.5}\text{TiO}_3$ . Експериментальні дані представлені у вигляді діаграм на комплексній площині ( $Z'$ - $Z''$ ) та обговорюються на підставі методу еквівалентних схем заміщення. Для вивченого температурно- частотного діапазону годографи містять дві дуги та описуються з використанням еквівалентної схеми, що складається з двох послідовно з'єднаних паралельних RC ланцюжків. Зсув центрів дуг вниз від осі  $Z'$ , обумовлений розподілом часів релаксації  $\tau$  імпедансу, враховано заміною звичайних ємностей узагальненими. Високочастотна дуга на годографах зіставлена провідності в об'ємі зразка. Низькочастотна дуга відображає перенесення заряду в приелектродних областях.

**Ключові слова:** натрий-висмутитовый титанат  $\text{Na}_{0.5}\text{Bi}_{0.5}\text{TiO}_3$ , импедансная спектроскопия, электропроводность.

### Introduction

Sodium bismuth titanate  $\text{Na}_{0.5}\text{Bi}_{0.5}\text{TiO}_3$  (NBT) and NBT - based solid solutions are intensively investigated as lead-free piezoelectric materials with high Curie temperature [1]. NBT belongs to the family of ferroelectric relaxors with  $A'_{1-x}A''_x\text{BO}_3$ -type perovskite structure. On cooling, NBT crystal undergoes the sequence of structural phase transitions: at  $T_C \approx 810\text{K}$  from cubic paraphase to the ferroelastic tetragonal phase; below  $T_R \approx 490\text{K}$  to rhombohedral ferroelectric phase [2, 3]. Probable statistical disordering of  $\text{Na}^+$  and  $\text{Bi}^{3+}$  ions in the A-position of the crystal lattice and structural defects formed by oxygen vacancies strongly influence physical properties of NBT. Heat treating NBT single crystals in the different

atmospheres made it possible to reveal the contribution of the structural defects, created by oxygen vacancies  $V_O^{\bullet\bullet}$ , to the permittivity and conductivity temperature behavior [4]. Thus, the low-frequency relaxation maximum of  $\epsilon$  near 670 K is associated with the presence of associated dipole complexes. Increase of conductivity at  $T > 700\text{K}$  is attributed to the formation of mobile defects [4, 5].

### Experimental results and discussion

It is known that the important information on charge transfer processes can be obtained by impedance spectroscopy [6, 7]. In this paper we study the spectra of complex impedance  $Z^*(\omega) = Z' - iZ''$  in order to elucidate

the mechanisms of charge transport in NBT single crystals.

The NBT single crystals were grown by Czochralskii method. Before the measurements the samples were annealed in air at 870K for 1h in order to destroy associated dipole complexes responsible for low-frequency dispersion of  $\epsilon$  near 670 K [5]. Samples were prepared as the plane-parallel plates with main faces parallel to the (001). Platinum electrodes were deposited by magnetron sputtering in an argon atmosphere. Studies of  $Z^*(\omega)$  spectra were carried out in the temperature interval 600-900 K and in the frequency range  $5 \cdot 10^5$  Hz by Tesla BM-507 impedance meter. Experimental data were obtained in the regime of thermal stabilization.

Impedance spectra  $Z^*(\omega)$  are presented as diagrams in the complex plane ( $Z'$ - $Z''$ ) on Fig. 1. For all temperatures studied the experimental hodographs consist of arcs of two semicircles. It is known [6, 7] that single arc in ( $Z'$ - $Z''$ ) plane can be described by the impedance of the parallel RC circuit  $Z^*(\omega) = Z(\omega = 0) \cdot [1 + i\omega\tau]^{-1}$ , where  $\omega$  – cyclic frequency of the measuring field;  $\tau=RC$  – relaxation time associated with the charge transfer rate. The hodographs consisting of two arcs are described by using

the equivalent circuit composed of two parallel RC circuits which are connected in series.

The centers of the arcs, plotted in Fig. 1, are shifted downward from  $Z'$  axis. Such shifts are usually explained as consequence of the relaxation time  $\tau=RC$  distribution in the sample volume and described by replacing ordinary capacities by frequency-dependent generalized ones  $C^*=A \times (i\omega)^{n-1}$  ( $0 \leq n \leq 1$ ) [7]. Considering the above, the experimental plots were described by using the equivalent circuit, which is shown in the inset to Figure 1 and has an impedance

$$Z^*(\omega) = \left[ (R_1^{-1} + i\omega C_1^*)^{-1} + (R_2^{-1} + i\omega C_2^*)^{-1} \right] \quad (1)$$

The hodographs, computed with the help of relation (1), are plotted in Figure 1 by solid lines.

According to [4] the charge transfer in NBT crystals combines the electronic and ionic components. Combination of electronic and ionic conductivity corresponds to a model of “parallel layers” [7, 8] and can be described by parallel connection of RC circuits, corresponding to the considered transfer mechanisms. It is clear, that parallel connection of several parallel RC-circuits is equivalent to single parallel RC-circuit with parameters averaged over existing

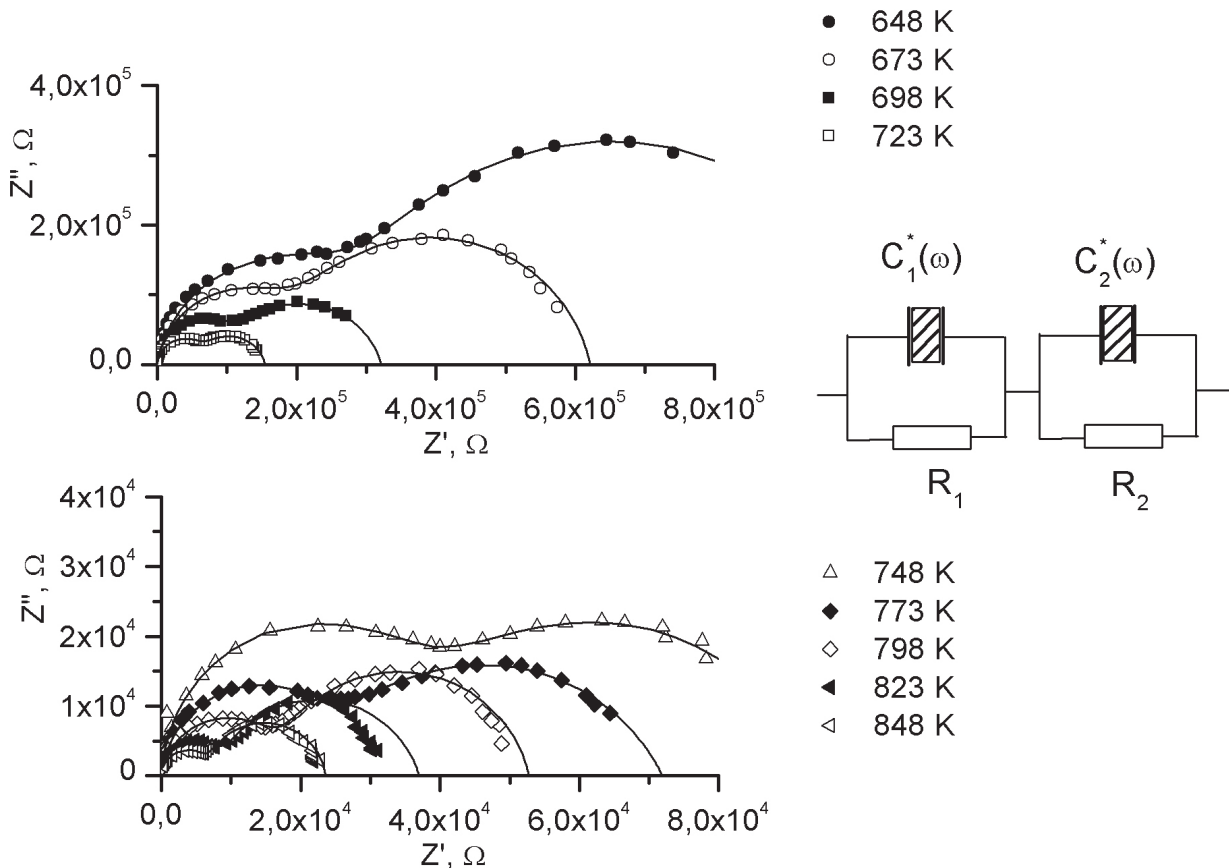


Fig. 1. Impedance spectra of NBT single crystals. Symbols represent experimental data. Solid lines are calculated by using impedance of equivalent circuit, shown in the inset.

conduction mechanisms.

Considering the above, presence of the two arcs on experimental hodographs (Fig. 1) requires to use the “series layers” model [8]. Therefore, the arcs on the hodographs in Fig. 1 can be compared with charge transfer in the sample volume and in the regions near of semitransparent electrodes. According to [8], to describe this situation the “series layers” model is applicable that corresponds to the serial connection of volume ( $Z_{\text{bulk}}$ ) and near-electrode ( $Z_{\text{nel}}$ ) impedances. Thus, the high-frequency semicircle on the hodograph in Figure 1 may be compared with the conductivity of the sample volume, which includes both electronic and ionic components. The low-frequency arc corresponds to the charge transfer in the near-electrode layer. The presence of the arc indicates that the electrodes are semitransparent for charge carriers. In the case of blocking electrodes accumulation of charge carriers in the near-electrode region leads to appearance of the vertical or inclined rays in the low-frequency part of the hodographs. Therefore, one can assume that the low-frequency arcs (Fig. 1) are contributed by electronic (or hole) conductivity.

It is known that the impedance (or conductivity) of the corresponding process in DC field may be determined by the intersection of the arc with the  $Z'$ -axis. Conductivity in zero frequency field, determined within this approach for high- and low-frequency arcs (Fig. 1), are presented in Arrhenius scale in Fig. 2. The inset in Fig. 2 shows the values of the index  $n$  in the expressions for generalized capacities used in (1). It is seen that the charge transfer processes corresponding to high-frequency and low-

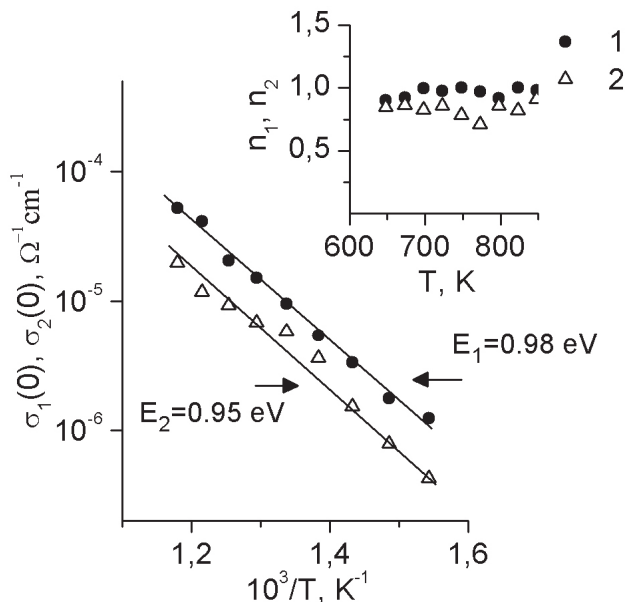
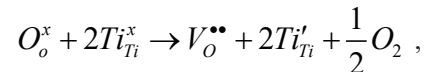


Fig. 2. Electrical conductivity in a DC field  $\sigma(\omega=0)$  vs  $1/T$ , determined from the hodographs in Fig. 1 for high-frequency (1) and low frequency (2) arcs. Inset shows the values of the generalized capacities index  $n$  used in the relation (1).

frequency arcs are characterized by similar values of the activation energy. The values of index  $n$  indicate that the distribution of the relaxation times  $\tau$  of charge transfer in near-electrode region (low-frequency arcs in Fig. 1) is significantly higher than in the bulk of the sample.

In [4] increase of the conductivity at  $T > 700$  K is explained by the formation of mobile defects associated with oxygen vacancies. Formation of vacancies  $V_{\text{O}}^{\bullet\bullet}$ , the charge of which is compensated by electrons localized in neighboring cations, is possible in the process of crystal growth. Quasi-chemical reactions of this process in the notation of Kroger-Wienke can be written as follows



where  $\text{O}_o^x$ ,  $\text{Ti}_{\text{Ti}}^x$  – filled neutral lattice sites;  $V_{\text{O}}^{\bullet\bullet}$  – oxygen vacancy  $\text{Ti}_{\text{Ti}}'$  –  $\text{Ti}^{4+}$  ion capturing an extra electron. In the external electric field electrons can hop over the sites, contributing to the electronic conductivity. The oxygen ions can hop through vacant sites ( $V_{\text{O}}^{\bullet\bullet}$ ) that determines ionic component of conductivity.

### Conclusions

Study of the complex impedance spectra showed that the experimental hodographs consist of arcs of two semicircles. The high-frequency arc is attributed to charge transfer in the sample volume. It is supposed that charge transfer in the bulk includes contributions from electronic and ionic hopping conductivity. Ionic conductivity can be result of oxygen vacancies  $V_{\text{O}}^{\bullet\bullet}$  motion. Electrons can hop via traps such as  $\text{F}^+$  centers. The low-frequency arc of experimental hodographs reflects electron conductivity in the near-electrode regions.

1. T. Takenaka, H. Nagata. Sodium Bismuth Titanate-Based Ceramics: Sodium Bismuth Titanate-Based Ceramics. In: Priya S, Nahm S, eds. Lead-Free Piezoelectrics, Springer, New York (2012), 255-290.
2. J.A. Zvirgzds, P.P. Kapostis, J.V. Zvirgzde, T.V. Kruzina. Ferroelectrics, 40, 75 (1982).
3. I.P. Pronin, P.P. Syrnikov, V.A. Isupov, V.M. Egorov, N.V. Zaitseva. Ferroelectrics, 25, 395 (1980).
4. T.V. Kruzina, V.M. Sidak, M.P. Trubitsyn, S.A. Popov and J. Suchanicz. Visnyk KhNU, 1076, 50 (2013).
5. T.V. Kruzina, V.M. Sidak, M.P. Trubitsyn, S.A. Popov and J. Suchanicz, Ferroelectrics, 462, 140 (2014).
6. R. West Solid state chemistry and its applications, John Wiley & Sons, New Yourk (1984), 336 p.
7. E. Barsoukov, J.R. Macdonald Impedance spectroscopy. Theory, experiment, and applications. Second Edition, John Wiley & Sons, Hoboken, New Jersey (2005), 595 p.

8. V.F. Lvovich Impedance spectroscopy. Application to electrochemical and dielectric phenomena, John Wiley & Sons, Hoboken, New Jersey (2012), 353p.
9. Ming Li at al. Chemistry of materials, 27, 629 (2015).